



SOLUTIONS OF THE MULTICHANNEL UNITARITY EQUATIONS
DESCRIBING THE ADDITION OF A RESONANCE AND BACKGROUND :
APPLICATION TO A POLE MODEL OF PHOTOPRODUCTION *)

M.G. Olsson **)
CERN - Geneva

A B S T R A C T

Addition of a resonance and background in the multichannel case is investigated. The generalization of a method, which correctly unitarizes a pole model of πN elastic scattering, is found. Application is made to photoproduction showing that a pole model can account for the resonant multipoles in the Δ region. The $\gamma N \Delta$ coupling constant required is nearly that predicted by the quark model.

*) Supported in part by the University of Wisconsin Research Committee with funds granted by the Wisconsin Alumni Research Foundation and in part by the U.S. Atomic Energy Commission under contract AT (11-1)-881.

**) Permanent address: Department of Physics, University of Wisconsin, Madison, Wisconsin 53706.

1. INTRODUCTION

The addition of two separately unitary amplitudes of the same partial wave has been discussed widely in the literature^{1,2)}. For a single open channel these methods all reduce to the addition of the phase shifts corresponding to each of the two amplitudes. A particularly important example occurs when one of the amplitudes is a resonance and the other a non-resonant background. In general, of course, it is difficult to separate an amplitude uniquely into these component parts, especially if the background is small and nearly real. There are cases, however, where this separation is quite clear. One example, which will be of particular importance in this paper, is the effective Lagrangian pole model. In this paper we will try to make the following points:

- i) There are a number of cases where the addition of phase shifts is not the correct procedure.
- ii) A correct method will be formulated for these cases valid for many open channels.
- iii) Application to elastic πN scattering will be reviewed. Photoproduction of pions will be calculated for the E_{1+} and M_{1+} multipoles and shown to agree well with experiment.

A partial wave dispersion relation can be written schematically as

$$\operatorname{Re} a(s) = B(s) + \frac{q^{2\ell}}{\pi} \int \frac{ds'}{q'^{2\ell}} \frac{\operatorname{Im} a(s')}{s' - s}, \quad (1)$$

where $B(s)$ contains all contributions except from the direct channel physical region. If the physical region considered is dominated by a single resonance we find that $\operatorname{Re} a(s) = B(s) + \operatorname{Re} a_{\text{res}}$. At the resonance position $s = s_r$, $\operatorname{Re} a_{\text{res}}(s_r) = 0$, so that,

$$\operatorname{Re} a(s_r) = B(s_r). \quad (2)$$

Here $B(s)$ will be considered to be a slowly varying background. In this paper, we shall require that the condition (2) be valid for any useful method of adding two amplitudes, at least in the limit of small real backgrounds.

For a single open channel the phase-shift addition method for combining a resonance and background can be expressed as

$$\begin{aligned}
 a(\omega) &= e^{i\delta} \sin \delta \equiv e^{i(\delta_r + \delta_b)} \sin(\delta_r + \delta_b) \\
 &= e^{i(\delta_r + \delta_b)} \left[e^{-i\delta_r} \sin \delta_b + e^{i\delta_b} \sin \delta_r \right] \\
 &= e^{i\delta_b} \sin \delta_b + e^{2i\delta_b} e^{i\delta_r} \sin \delta_r
 \end{aligned}$$

or

$$a(\omega) = a_b(\omega) + e^{2i\delta_b} a_r(\omega). \quad (3)$$

Taking the real part we find

$$\text{Re } a(\omega) = B(\omega) + \text{Re} \left[e^{2i\delta_b} a_r(\omega) \right]. \quad (4)$$

Comparing Eq.(4) with the dispersive condition (2), we see that for small background phase shifts at resonance

$$\text{Re } a(\omega_r) = -B(\omega_r).$$

Hence phase-shift addition does not obey the dispersive condition (2).

It is clear from Eq.(4) that the only way that the dispersive condition (2) can be realized is if the phase $e^{2i\delta_b}$ is absent as a multiplicative factor of the resonance amplitude. There are two apparent possibilities for accomplishing this:

- i) Modification of the background term.
- ii) Modification of the resonance propagator.

The first possibility can be rejected, since a simple phase modification of the background term leads back again to the phase-shift addition result. Since the background is unitary by itself outside the resonance region, it is perhaps more satisfying to modify the resonance term in any case. Modification of the resonance denominator has been considered first by De Baenst et al.³⁾, using a non-unitary background, and later by the present author⁴⁾ with the simplifying assumption of a separately unitary background. This method has the virtue of satisfying the dispersive condition (2) and since the background terms of an effective Lagrangian pole model can be easily identified with the dispersive ones⁵⁾

this unitarization method is the proper one to use when applying a pole model.

In Section 2 we consider resonance and background addition in the multichannel situation. Application to elastic πN scattering is reviewed in Section 3 and in Section 4 the case of photoproduction is discussed. It is shown in this latter section that the resonant multipoles are correctly described using a simple pole model.

2. SOLUTIONS TO THE MULTICHANNEL UNITARITY EQUATIONS

2.1 General solution

A partial wave amplitude a_{ij} is assumed to satisfy the unitarity equation ²⁾

$$\text{Im } a_{ij} = \sum_k a_{ik} \rho_k a_{kj}^* \quad , \quad (5)$$

where ρ_k is a phase-space factor^{*)}. We shall consider a_{ij} as the sum of a background amplitude b_{ij} and a resonance amplitude r_{ij} .

$$a_{ij} = b_{ij} + r_{ij} \quad . \quad (6)$$

The background amplitude will be assumed to be separately unitary and to satisfy

$$\text{Im } b_{ij} = \sum_k b_{ik} \rho_k b_{kj}^* \quad . \quad (7)$$

Putting Eq. (6) into Eq. (5) and using Eq. (7) we find

$$\text{Im } r_{ij} = \sum_k \left\{ r_{ik} \rho_k r_{kj}^* + r_{ik} \rho_k b_{kj}^* + b_{ik} \rho_k r_{kj}^* \right\} \quad . \quad (8)$$

We shall assume a factorizing resonance amplitude,

*) We always take $\rho_i = p_i \theta(s - s_{th})$ for two particle states where p_i is the c.m. momentum and s_{th} is the threshold energy.

$$r_{ij} = v_i e^{i\phi_i} P v_j e^{i\phi_j} \quad (9)$$

and by defining

$$\begin{aligned} P^{-1} &\equiv (\epsilon - i\gamma) \sum_k v_k^2 \rho_k \\ \beta_{ij} &\equiv \frac{v_j}{v_i} \rho_j b_{ij} \end{aligned} \quad (10)$$

and simplifying by making use of $P = |P|^2 P^{-1*}$, we find that the unitarity equations (8) become

$$\begin{aligned} \text{Im} \left[e^{i(\phi_i + \phi_j)} (\epsilon + i\gamma) \right] &= e^{i(\phi_i - \phi_j)} + \\ &(\epsilon + i\gamma) e^{i\phi_i} \sum_k \beta_{jk}^* e^{i\phi_k} + (\epsilon - i\gamma) e^{-i\phi_j} \sum_k \beta_{ik} e^{-i\phi_k} \end{aligned} \quad (11)$$

The solution to this set of equations is of the form

$$\sin \phi_i = \left(\sum_k \beta_{ik} e^{-i\phi_k} \right) - F_i \quad (12)$$

Substituting Eq.(12) into the system of equations (11) and solving for γ we obtain

$$\gamma = \frac{1 + \epsilon (F_i e^{-i\phi_i} + F_j^* e^{i\phi_j})}{1 + i (F_i e^{-i\phi_i} - F_j e^{i\phi_j})} \quad (13)$$

Since by our factorization hypothesis (9) we have assumed that γ is independent of any channel index, we must take

$$F_i = G e^{i\phi_i} \quad (14)$$

The factor G is related to some scalar quantity associated with the background matrix b_{ij} . Substituting the scalar requirement (14) into the solution for γ in Eq.(13) we find

$$\gamma = \frac{1 + 2\varepsilon \operatorname{Re} G}{1 - 2 \operatorname{Im} G} . \quad (15)$$

In order to solve for G we must discuss firstly the properties of F_i as defined by Eq.(12).

Since the background amplitude b_{ij} satisfies the unitarity equation (7), the matrix β_{ij} defined by Eq.(10) must satisfy a similar equation

$$\operatorname{Im} \beta_{ij} = \sum_k \beta_{ik} \beta_{kj}^* . \quad (16)$$

By separating Eqs.(12) and (16) into real and imaginary parts we find that F_i must obey the following consistency condition^{*)}:

$$\operatorname{Im} F_i = \sum_k \beta_{ik}^* F_k . \quad (17)$$

When this condition is applied to the scalar condition (14) we find that G must satisfy

$$\operatorname{Im} G = |G|^2 . \quad (18)$$

*) The consistency condition of Eq. (17) ensures that these are the right numbers of equations to determine $\{\phi_i\}$. Since the equations are trigonometric there still may be cases where there are no solutions. This is not generally the case; however in the extreme case of only one strong channel there may be no solutions if the backgrounds are too large. We shall see this in detail in Section 4 where we investigate photoproduction.

Of course, we can trivially satisfy Eq. (18) by taking $G = 0$. The set of equations for ϕ_i is then

$$\sin \phi_i = \sum_k \beta_{ik} e^{-i\phi_k}$$

and the solution for γ from Eq. (15) is

$$\gamma = 1.$$

This solution is the usual²⁾ one which reduces to phase-shift addition in the single channel case. We have seen that this sort of solution is not consistent with the dispersive constraint (2) so we must reject the $G = 0$ solution.

Since the trace of β_{ij}

$$T = \sum_k \beta_{kk}$$

is a scalar we might try G proportional to T . The choice

$$G = \left[\frac{\text{Im} T}{|T|^2} \right] T \quad (19)$$

satisfies the constraint (18) that $\text{Im} G = |G|^2$. As we shall see, this choice for G generalizes the one channel result⁴⁾ which satisfies the dispersive constraint (2).

The scattering amplitude is finally given by Eqs. (6), (9), and (10) to be

$$a_{ij} = \frac{v_i}{v_j \rho_j} \left[\beta_{ij} + \left(\frac{v_i^2 \rho_i}{\sum_k v_k^2 \rho_k} \right) \frac{e^{i(\phi_i + \phi_j)}}{\epsilon - i\gamma} \right]. \quad (20)$$

The vertex functions v_i are assumed to be specified, for example, by a pole model and the phases ϕ_i are found by solving Eqs. (12), (14), (19).

2.2 Single open channel

For the case of one open channel we can show that our results reproduce the solution described in our previous work⁴⁾. Since the background is by itself unitary we must take

$$\beta = \rho b = e^{i\delta_e} \sin \delta_e ,$$

where δ_e is the elastic background phase shift. From Eq. (19) we have

$$G = \beta$$

and by Eq. (15)

$$\gamma = \frac{1 + \epsilon \sin 2\delta_e}{\cos 2\delta_e} . \quad (21)$$

The solution for ϕ follows from Eq. (12):

$$\sin \phi = \beta e^{-i\phi} - \beta e^{i\phi} = -2i\beta \sin \phi .$$

The solutions are $\phi = 0$ and π . The latter can be rejected, since the original resonance amplitude must remain when $\beta = 0$; hence we have

$$\phi = 0 .$$

The elastic amplitude is from Eq. (20)

$$\rho a = e^{i\delta} \sin \delta = \frac{1}{\epsilon - i\gamma} + e^{i\delta_e} \sin \delta_e . \quad (22)$$

Solving for δ gives (after some algebra)

$$\cot \delta = \frac{\epsilon + \tan \delta_e}{1 + \epsilon \tan \delta_e} . \quad (23)$$

This is precisely the solution used previously⁴⁾ (with $\tan \delta_e = B$).

2.3 Weak background limit

In many cases the non-resonant background is to a good approximation small and real. Since the β_{ik} are now small we expect ϕ_i also to be small. To first order in β_{ik} we take from Eqs. (12), (19)

$$\begin{aligned}
 \phi_i &= \sum_k (\beta_{ik} - \beta_{kk}) \\
 G &= \sum_k \beta_{kk} \\
 \gamma &= 1 + 2\epsilon G.
 \end{aligned}
 \tag{24}$$

The amplitude is then, from Eq. (20),

$$a_{ij} = \frac{v_i}{v_j \rho_j} \left[\beta_{ij} + \left(\frac{v_i^2 \rho_i}{\sum_k v_k^2 \rho_k} \right) \frac{e^{i(\phi_i + \phi_j)}}{\epsilon - i\gamma} \right].
 \tag{25}$$

In the case where there is only one strong channel (call it channel j), Eq. (25) simplifies to

$$a_{ij} = \frac{v_i}{v_j \rho_j} \left[\beta_{ij} + \frac{e^{i\phi_i}}{\epsilon - i\gamma} \right],
 \tag{26}$$

since by Eqs. (24) $\phi_j = 0$ and $\gamma = 1 + 2\epsilon\beta_{jj}$.

3. ELASTIC πN SCATTERING

In this section we review the application^{3,4,6,7)} of a pole model to the calculation of the (3,3) phase shift. As we shall see, the pole model when properly unitarized accounts nicely for the momentum dependence of the (3,3) phase shift once the resonance position and $\pi N\Delta$ coupling constant are fixed.

As has been pointed out by several authors, a naïve application of the pole model³⁾ cannot account for the observed δ_{33} phase shift without the introduction of various form factors⁸⁾, which is equivalent to the insertion of an arbitrary momentum dependent width and eliminating any predictive power of the model. However, De Baenst et al.³⁾ and Höhler et al.⁶⁾ have shown that, when the pole model resonance amplitude is added to a nucleon exchange Born term background, a result in agreement with experiment is obtained and the necessary pole model parameters are consistent with those employed in other kinematic regions.

A general $\pi N \Delta$ interaction with gradient coupling is^{6,7,9)}

$$\mathcal{L} = g^* \bar{\Delta}_\mu \otimes_{\mu\nu} N \partial_\nu \pi + \text{h.c.} \quad (27)$$

with

$$\otimes_{\mu\nu} = \delta_{\mu\nu} + \left[\frac{1}{2}(1+4Z)A + Z \right] \gamma_\mu \gamma_\nu, \quad (28)$$

where Z is an arbitrary parameter and A is the parameter appearing in the spin $\frac{3}{2}$ propagator⁷⁾. Using the Δ propagator and the interaction (27) the Δ exchange contribution can be calculated⁷⁾. The invariant amplitudes depend on the coupling constant g^* and the parameter Z only.

If the isospin $\frac{3}{2}$, $J^P = \frac{3}{2}^+$ partial wave is now projected out we obtain

$$a = \frac{M_r \Gamma_\Delta / q}{M_r^2 - \Delta} + \text{u-channel contribution} \quad (29)$$

where^{*)}

$$\Gamma_\Delta = \frac{g^{*2}}{4\pi} \frac{(E+M)(W+M_r)}{6\Delta} \frac{q^3}{q} .$$

The u-channel contribution is slowly varying in the resonance region and can be shown to be less than 5 per cent of the dominant N exchange contribution in this partial wave.

A naïve application of the pole model would be to neglect not only the u-channel Δ exchange contribution but also all other possible backgrounds. From Eq. (29) the pole model expression for the (3,3) amplitude is

$$q a = \frac{M_r \Gamma_\Delta}{M_r^2 - \Delta} \equiv \frac{1}{\epsilon} . \quad (30)$$

*) The kinematic quantities have their usual meaning: M_r is resonance mass; M is nucleon mass; q is c.m. momentum; $\omega^2 = q^2 + 1$; $W^T = \sqrt{s}$ total c.m. energy, $E = W - \omega$; unless otherwise specified we use natural units.

An obvious way to avoid both the pole on the real axis and to saturate elastic unitarity at resonance would be to insert the factor $-iM_r \Gamma_\Delta(s)$ in the denominator giving

$$\frac{g_a}{\delta} = \frac{M_r \Gamma_\Delta}{M_r^2 - s - iM_r \Gamma_\Delta} = \frac{1}{\varepsilon - i} \quad (31)$$

The experimental (3,3) phase shift δ_{33} can be parametrized¹⁰⁾ as

$$\tan \delta_{33} = \frac{M_0 \Gamma(\Delta)}{M_0^2 - s} \quad (32)$$

$$\Gamma(\Delta) = \Gamma_0 \left(\frac{1 + (Rq_0)^2}{1 + (Rq)^2} \right) \left(\frac{q}{q_0} \right)^3,$$

where $\Gamma_0 = 111$ MeV and $M_0 = 1231$ MeV.

By fixing the pole model parameters M_r and g^* such that the phase-shift and phase-shift slope have their experimental values we can test the momentum dependence of this naïve pole model. Comparing Eqs. (31) and (32) at the resonance energy we find

$$M_r = 1231 \text{ MeV}$$

$$\Gamma_\Delta(M_r) = \Gamma_0 \quad (33)$$

so that

$$\frac{g^*{}^2}{4\pi} = 0.365.$$

The predicted momentum dependence of the naïve pole model is shown by the dashed curve in Fig. 1. The phase-shift predictions are poor, especially above resonance. Furthermore, the mass and coupling constant are in poor agreement with those obtained by other means⁶⁾.

A better way of calculating the (3,3) phase shift with a pole model is to add to the resonance amplitude any non-resonant background required by the pole model. The question of how to add the resonance and background has been dealt with in the previous sections. The largest of the backgrounds required by the

pole model comes from N exchange. Two-pion exchange in $I = 0$ also gives an appreciable background contribution approximately 25% of the N exchange background at low energies⁴⁾. Unfortunately, in the absence of an *a priori* knowledge of the σ -term and its dependence upon momentum transfer a reliable calculation of the $\pi\pi$ $I = 0$ exchange contribution is not possible. In our previous work⁴⁾ we used a model due to Schnitzer^{7,11)} with some simplifying assumptions to estimate this σ -term contribution at low energies. The resulting background was used to predict the momentum dependence of the (3,3) phase shift. In this paper we shall take a different approach. We shall use Eq. (23) to fix the parameters M_r and g^* independently of the size of the background. The background required to account for the observed phase shift can then be calculated at each energy.

From Eq. (23) we note that at $\epsilon = \pm 1$ the phase shift is 45° and 135° , respectively, independent of the background. If we denote s_+ and s_- to be the values of s when $\epsilon = \pm 1$ we have the two equations

$$M_r^2 - s_+ = M_r \Gamma_\Delta(s_+)$$

$$M_r^2 - s_- = -M_r \Gamma_\Delta(s_-) ,$$

where

$$\Gamma_\Delta(s) = \frac{g^{*2}}{4\pi} C(s, M_r) , \quad C(s, M_r) = \frac{(E+M)(W+M_r)}{6s} g^3 .$$

Solving for g^* we find

$$\frac{g^{*2}}{4\pi} = \frac{(s_- - s_+)/M_r}{C(s_+, M_r) + C(s_-, M_r)} . \quad (34)$$

The resonant mass M_r is then

$$M_r^2 = s_+ + M_r \Gamma_\Delta(s_+, M_r) . \quad (35)$$

Since g^* is not very sensitive to M_r , the solution can easily be found by iterating Eqs. (34) and (35). Once the resonance parameters are found the background can be deduced from Eq. (23) to be

$$B(\Delta) = \tan \delta_e = \frac{\cot \delta - \epsilon}{1 - \epsilon \cot \delta} , \quad (36)$$

where δ is the experimental (3,3) phase shift¹⁰⁾.

The phase-shift analysis of Carter et al.¹⁰⁾ determined δ_{33} for the two charge states Δ_{++} and Δ_0 . These two phase shifts are slightly different reflecting isospin breaking. For the Δ_{++} case derived from $\pi^+ p$ scattering the phase shifts are more accurately determined. The energies for $\delta_{33} = 45^\circ$ and 135° are, respectively, in this case

$$\begin{aligned} W_+ &= 1190.0 \pm 4 \text{ MeV} \\ W_- &= 1314.0 \pm 2 \text{ MeV} . \end{aligned}$$

The resulting resonance parameters are

$$\begin{aligned} M_r^{++} &= 1218.2 \text{ MeV} \\ \frac{g^{*2}}{4\pi} &= 0.31 . \end{aligned} \quad (37)$$

The background required to give the experimental phase shifts is calculated from Eq. (36) and displayed in Fig. 2. For comparison with the Δ_0 case the background at resonance ($\delta = 90^\circ$) is

$$B^{++}(\Delta_0^{++}) = 0.26 .$$

For the corresponding case of the Δ_0 phase shift extracted from $\pi^- p$ scattering, we find

$$\begin{aligned} M_r^0 &= 1220 \text{ MeV} \\ \frac{g^{*2}}{4\pi} &= 0.31 \\ B^0(\Delta_0^0) &= 0.25 \end{aligned} \quad (38)$$

Thus the isospin breaking is manifested in the 2 MeV mass shift and a slight decrease of the background in the neutral case. The former is expected by comparison

with other decuplet mass differences and the latter implies that the πNN coupling constant is isospin broken by a small factor.

We shall finally try to account for the observed coherent background in Fig. 2. The N exchange contribution can be calculated from the πNN interaction^{6,7)}

$$\mathcal{L} = if \bar{N} \gamma_\mu \gamma_5 N \partial_\mu \pi , \quad (39)$$

where f is the rationalized coupling constant¹³⁾

$$\frac{f^2}{4\pi} = 0.079 \pm 0.001 . \quad (40)$$

This axial-vector Born term differs only by a constant from the usual pseudo-scalar Born term and thus gives the same (3,3) partial wave projection. The N exchange background in this partial wave is given by

$$g a_N = B_N = \frac{f^2}{4\pi} \frac{1}{8WM^2 g} \left[(E+M)(W-M) Q_1(\zeta) - (E-M)(W+M) Q_2(\zeta) \right] \quad (41)$$

where

$$\zeta = \frac{2WE-1}{2g^2} .$$

A plot of B_N in the Δ resonance region is shown by the curve in Fig. 2. As can be seen from Fig. 2, the N exchange contribution accounts for about 80% of the observed background. As was pointed out in our previous work⁴⁾, the remainder is easily accounted for by a δ -term contribution of reasonable size.

The resonance parameters M_Δ and g^* that we have found necessary to account for the (3,3) phase shift are consistent with those used by pole models to account for the entire πN amplitude in the threshold region^{6,7)}. The resonance energy must fall below the $\delta = 90^\circ$ point and g^* must be less than that given by the naïve application of the pole model. Hence the same set of pole model parameters suffice to fit data above as well as below threshold when the model is unitarized properly. We shall next apply the pole model to photoproduction in the Δ region. Again the pole model will prove adequate in explaining the M_{1+} and E_{1+} multipoles with the introduction of one new coupling constant which will turn out to have nearly the quark model value.

4. PHOTOPRODUCTION

An interesting example of the application of our methods to the multichannel case is that of single pion production by photons at low energy. In this case, the first channel is $\gamma N \rightarrow \gamma N$, and above photoproduction threshold we must couple this to elastic $\pi N \rightarrow \pi N$ which we denote by channel two.

Since v_1 and b_{12} are proportional to e , the electric charge, and b_{11} to e^2 , we can neglect β_{11} and β_{21} compared to β_{12} and β_{22} . The β_{ij} must satisfy the unitarity conditions (16), which give

$$\begin{aligned} \text{Im } \beta_{12} &= \beta_{12} \beta_{22}^* \\ \text{Im } \beta_{22} &= |\beta_{22}|^2 . \end{aligned}$$

From the second equation we take

$$\beta_{22} = e^{i\delta_e} \sin \delta_e$$

and from the first we find

$$\beta_{12} = |\beta_{12}| e^{i\delta_e} . \quad (42)$$

The later relation is just "Watson's theorem"¹⁴⁾. By Eq. (19) we have, as in the elastic case,

$$G = \beta_{22} = e^{i\delta_e} \sin \delta_e .$$

The system of equations for the phase angles ϕ_i is, from Eqs. (12), (14),

$$\begin{aligned} \sin \phi_1 &= \beta_{12} e^{-i\phi_2} - e^{i\delta_e} \sin \delta_e e^{i\phi_1} \\ \sin \phi_2 &= \beta_{22} e^{-i\phi_2} - e^{i\delta_e} \sin \delta_e e^{i\phi_2} . \end{aligned}$$

The second equation is the same as in the single channel case, so that $\phi_2 = 0$.
The first equation then becomes

$$\sin \phi_1 = |\beta_{12}| e^{i\delta_e} - \sin \delta_e e^{i(\phi_1 + \delta_e)}.$$

If we define

$$\sin \delta_p \equiv |\beta_{12}|, \quad (43)$$

we see that that the solution for ϕ_1 is ^{*)}

$$\phi_1 = \delta_p - \delta_e. \quad (44)$$

Since G is the same as in the elastic case, γ will also be [from Eq. (21)]

$$\gamma = \frac{1 + \epsilon \sin 2\delta_e}{\cos 2\delta_e}$$

The photoproduction amplitude is given by Eq. (20) to be

$$a_{12} = \frac{v_1}{v_2 \rho_2} \left[\beta_{12} + \frac{e^{i\phi_1}}{\epsilon - i\gamma} \right], \quad (45)$$

where we have again neglected $\rho_1 v_1^2$ compared to $\rho_2 v_2^2$. We can put this amplitude into a form which explicitly exhibits Watson's theorem for the whole amplitude. Through Eq. (22) the elastic amplitude is given by

$$e^{i\delta} \sin \delta = \frac{1}{\epsilon - i\gamma} + e^{i\delta_e} \sin \delta_e.$$

*) For $|\beta_{12}| > 1$ there is no real solution for ϕ_1 . It is interesting to note, as we shall see, that in the case of the E_{1+} multipole $|\beta_{12}|$ is nearly unity.

By adding and subtracting we find

$$a_{12} = \frac{v_1}{v_2 \rho_2} \left[e^{i\phi_1} e^{i\delta} \sin \delta + \sin \phi_1 \right],$$

which can be rewritten as

$$a_{12} = N e^{i\delta} \sin(\delta + \phi_1), \quad (46)$$

where

$$\phi_1 = \delta_p - \delta_e \quad \text{and} \quad N = \frac{v_1}{v_2 \rho_2}.$$

It should be mentioned that a_{12} can refer to either the M_{1+} or E_{1+} multipole moments. Although a_{12} has the phase of the elastic πN amplitude, the imaginary part will be maximum at a lower energy if ϕ_1 is positive. This downward shift is observed to some extent in the M_{1+} multipole¹⁵⁾ and it is very pronounced in the E_{1+} multipole.

4.1 Resonance vertex factors

In an effective Lagrangian pole model the vertex factors v_i are uniquely defined for a given resonance. In the elastic case the interaction (28) gave the elastic resonance amplitude to be

$$a_{22} = \frac{v_2^2}{M_r^2 - \Delta} = \frac{M_r \Gamma_\Delta(\Delta)/g}{M_r^2 - \Delta},$$

and hence

$$v_2^2 = \frac{g^*{}^2}{4\pi} \frac{M_r(E+M)(W+M_r)}{6\Delta} \frac{1}{b^2}. \quad (47)$$

For the photoproduction resonance multipole vertex factors we follow the work of Peccei¹⁶⁾ who uses the $\gamma N \Delta$ interaction

$$\mathcal{L} = -\frac{e\chi g^*}{2M} \bar{\Delta}_\mu \gamma_\nu F_{\mu\nu} N + \text{h.c.} \quad (48)$$

where an additional coupling which does not contribute to the M_{1+} and E_{1+} multipoles has been neglected. The projections of the resulting invariant amplitudes¹⁶⁾ into the M_{1+} and E_{1+} multipoles¹⁷⁾ for the direct channel resonance part results in

$$\begin{Bmatrix} M_{1+} \\ E_{1+} \end{Bmatrix} = \frac{v_1 v_2}{M_r^2 - \Delta} \quad , \quad (49)$$

where*)

$$v_1 v_2 = \frac{e\chi g^* k q}{96\pi W M} \left(\frac{W+M_r}{W+M} \right) \Delta_1 \Delta_2 \begin{Bmatrix} 3W+M \\ -(W-M) \end{Bmatrix}$$

The particular combination of vertex functions needed for Eq. (46) is then from Eqs. (47), (49)

$$\mathcal{N} = \frac{v_1}{v_2 \rho_2} = \frac{e\chi g^* k W \Delta_1}{4g^* M M_r (W+M) q^2 \Delta_2} \begin{Bmatrix} 3W+M \\ -(W-M) \end{Bmatrix} \quad (50)$$

where the upper quantity in the brackets is relevant for M_{1+} and the lower for E_{1+} .

*) The kinematic quantities for photoproduction are: $k = \text{c.m. incident momentum}$;
 $E_1 = \sqrt{k^2 + M^2}$; $s_1 = \sqrt{E_1 + M}$; $s_2 = \sqrt{E_1 - M}$; $e^2/4\pi = 137$ and $f^2/4\pi = 0.079$.

4.2 Born term multipoles

Using the results of Peccei¹⁶⁾, the invariant amplitudes for the Born terms in isospin $\frac{3}{2}$ are

$$A_1 = \frac{ef}{2} \left[\frac{-4M}{M^2-u} + \frac{2\chi}{M} \right]$$

$$A_2 = \frac{ef}{2} \left[\frac{-8M}{(1-t)(M^2-u)} \right]$$

$$A_3 = -A_4 = \frac{ef}{2} \left[\frac{-4\chi}{M^2-u} \right] ,$$

where

$$\chi = \frac{1}{2} (\mu_p - \mu_n) = 1.85 .$$

The Born term multipole projections¹⁷⁾ can now be calculated and the relevant M_{1+}^B and E_{1+}^B multipoles are plotted in Fig. 3. The constant term in the first invariant amplitude arises from the current algebra constraint¹⁸⁾ and does not contribute to the M_{1+} and E_{1+} multipoles. The other contributions to the background in these multipoles comes primarily from Δ exchange. The effect of Δ exchange is to increase the magnitude of the background by about 10% in each case.

The quantity δ_p has been defined in Eq. (43) as

$$\delta_p = \sin^{-1} \beta_{12} = \sin^{-1} \left[\frac{M^B}{N} \right] \quad (51)$$

for each of the multipoles M_{1+} and E_{1+} . In Eq. (51) M^B denotes the background multipole projection.

4.3 Prediction of the resonant multipoles

The only new parameter which we have introduced in our pole model of resonant photoproduction is κ^* , the $\gamma N \Delta$ coupling constant. We shall fix the value of κ^* using the value of the M_{1+} multipole at resonance. The momentum dependence of the M_{1+} multipole and the normalization and momentum dependence of the much smaller E_{1+} multipole are then predicted.

The value of κ^* which we shall choose is

$$\chi^* = 4.33 \quad (52)$$

In Figs. 3 we plot the quantity N for the M_{1+} and E_{1+} multipoles from Eq. (50). Using the values of N and the Born pole multipole projections from Figs. 3, we calculate the phase angles δ_p from Eq. (51) which are displayed for each multipole in Fig. 4. Using the N exchange background of Fig. 2 we now compute the phases $\phi_1 = \delta_p - \delta_e$ (where $\tan \delta_e = B_N$), which are also displayed in Fig. 4. The resonant multipole can now be calculated from Eq. (46)

$$\begin{aligned} M_{1+} &= N_M e^{i\delta} \sin(\delta + \phi_1^M) \\ E_{1+} &= N_E e^{i\delta} \sin(\delta + \phi_1^E) \end{aligned} \quad (53)$$

with the aid of the elastic resonant phase shift δ given by Fig. 1.

The results for the M_{1+} multipole are shown in Fig. 5. The predictions are compared with the energy independent multipole analysis of Noelle, Pfeil, and Schwela¹⁵⁾. We first note that the maximum of $\text{Im } M_{1+}$ is shifted about 6 MeV lower in energy than the elastic resonance position. This follows directly from Eq. (53), since ϕ_1^M is about 6 degrees at resonance. Although ϕ_1^M is small it plays an important role in the M_{1+} multipole. For example, at $W = 1300$ MeV, if we set $\phi_1^M = 0$ we would obtain $\text{Re } M_{1+} = -14.9$ and $\text{Im } M_{1+} = 17.4$ compared to $\text{Re } M_{1+} = -13.3$ and $\text{Im } M_{1+} = 15.5$ in the actual case.

First in SU(6) and the quark model¹⁸⁾, and more recently in the constituent-current quark transformation scheme¹⁹⁾, the transition magnetic moment for $\Delta \rightarrow N\gamma$ is predicted to be

$$\mu^* = \frac{2\sqrt{2}}{3} \mu(\text{proton}) .$$

By comparison of the partial widths in Dalitz and Sutherland¹⁸⁾ with the expressions in Eq. (49), we find that the corresponding value of the $\Upsilon\Delta$ coupling constant is

$$\chi^* = 4.0 .$$

As we have seen, the value $\kappa^* \approx 4.33$ gives a good representation of the M_{1+} multipole. The indicated symmetry-breaking is less than 10%, a number considerably less than the 28% breaking originally found¹⁸⁾. Part of the difference comes from the smaller value of g^* as discussed in Section 3. The remaining difference probably comes from the neglect of E_{1+} M_{1+} interference (in the angular distributions) in the analysis of Dalitz and Sutherland¹⁸⁾.

Once the value of κ^* is fixed, the E_{1+} multipole is apparently uniquely specified. From Eq. (53) the real and imaginary parts of E_{1+} are calculated and the result is shown in Fig. 6. As in the magnetic case we compare the prediction with the multipole analysis of Noelle et al¹⁵⁾. There is an important difference, however, between the M_{1+} and E_{1+} cases. From Fig. 3 we see that N_E is nearly equal to E_{1+}^B , whereas N_M exceeds the Born projection M_{1+}^B by about a factor of two. The result of this can be seen in Fig. 4; δ_p^M is considerably smaller than δ_p^E , the latter approaching the limiting value of $\delta_p \leq 90^\circ$. The angle δ_p^E and hence ϕ_1^E is thus very sensitive to the exact value of κ^* and the magnitude of the background. If we include the Δ exchange contribution E_{1+}^B will increase in magnitude by about 0.2, resulting in a δ_p^E of nearly 90° . This would cause qualitative changes in the curves on Fig. 6. $\text{Im } E_{1+}$ will peak at a lower energy and fall rapidly above resonance due to the $\sin(\delta + \phi_1^E)$ factor and can even have a zero above resonance. In $\text{Re } E_{1+}$ a corresponding second zero will appear. Thus we see that the E_{1+} multipole is quite sensitive to details of the pole model because the background term is so large. It will be interesting to see whether this maximal background is found in other processes, for example in Compton scattering. The pole model can also be applied quite successfully to the entire photoproduction amplitude in all charge states in the Δ region²⁰⁾.

5. CONCLUSIONS

We have seen that a pole model can be unitarized in a manner consistent with dispersion relations. The addition of a resonance and a background term in this manner is valid for the multichannel case. In two cases the unitarized pole model is shown to be quite successful. Elastic πN scattering in the (3,3) partial wave and resonant photoproduction multipoles have straightforward interpretations in terms of a simple pole model consisting of a Δ resonance and a non-resonant background in the same partial wave. The background comes from the partial wave projection of other pole processes, dominantly the Born terms. The effect of the background in elastic πN scattering is to modify the rapid energy dependence of the pole-model resonance vertices. In photoproduction, the background further distorts the resonance shape. In the electric quadrupole case this distortion is extreme and probably maximal. The $\Upsilon N \Delta$ coupling constant required is that predicted from the quark model to within 10%.

The resonant mass and $\pi N\Delta$ coupling constant required to fit the (3,3) phase shift are the same as used in a general pole model fit to the scattering lengths or to the crossing symmetric expansion parameters below threshold^{6,7)}. In photo-production the $\gamma N\Delta$ coupling constant is nearly that predicted by the quark model. We see that a properly unitarized pole model provides a simple, coherent and accurate picture of low-energy scattering, at least in the two cases discussed here.

I would like to thank Dr. C. Michael for several discussions and Professor E.T. Osypowski for collaboration in closely related work.

REFERENCES

- 1) Robert K. Adair, Phys. Rev. 113, 338 (1959);
R.H. Dalitz, Annu. Rev. Nuclear Sci. 13, 339 (1963);
C.J. Goebel and K.W. McVoy, Phys. Rev. 164, 1932 (1967).
- 2) C. Michael, Phys. Letters 21, 93 (1966).
- 3) A. De Baenst-Vandenbrouke and P. De Baenst, On the isobar model parameters of the first pion-nucleon resonance, preprint, Mathematical Physics Department, University College Dublin (1973).
- 4) M.G. Olsson, CERN preprint TH.1811 (1974).
- 5) D. Amati and S. Fubini, Annu. Rev. Nuclear Sci. 12, 359 (1962).
- 6) G. Höhler, H.P. Jakob and R. Strauss, Nuclear Phys. B39, 237 (1972).
- 7) M.G. Olsson, Leaf Turner and E.T. Osypowski, Phys. Rev. D7, 3444 (1973).
- 8) H. Pilkuhn and A. Swoboda, Nuovo Cimento Letters 1, 854 (1969).
- 9) L.M. Nath, B. Etemadi, and J.D. Kimel, Phys. Rev. D3, 2153 (1971).
- 10) J.R. Carter, D.V. Bugg and A.A. Carter, Nuclear Phys. B58, 378 (1973);
Particle Data Group (1972), Phys. Letters 39 B, 1 (1972).
- 11) H.J. Schnitzer, Phys. Rev. D5, 1482 (1972); Phys. Rev. D6, 1801 (1972).
- 12) M.G. Olsson, Phys. Rev. Letters 14, 118 (1965).
- 13) D.V. Bugg, A.A. Carter and J.R. Carter, Rutherford preprint (1973).
H. Pilkuhn, W. Schmidt, A.D. Martin, C. Michael, F. Steiner, B.R. Martin,
M.M. Nagels, J.J. De Swart, Nuclear Phys. B65, 460 (1973).
- 14) K.M. Watson, Phys. Rev. 95, 228 (1954);
A. Donnachie, High energy physics V (ed. E.H.S. Burhop) (Academic Press,
New York, 1972), p. 1.
- 15) P. Noelle, W. Pfeil, and D. Schwela, Nuclear Phys. B26, 461 (1971);
W. Pfeil and D. Schwela, Nuclear Phys. B45, 379 (1972).
- 16) R.D. Peccei, Phys. Rev. 181, 1902 (1969).
- 17) James Stutsman Ball, Phys. Rev. 124, 2014 (1961).
- 18) R.H. Dalitz, and D.G. Sutherland, Phys. Rev. 146, 1180 (1966).
- 19) J. Weyers, Lectures given at the International Summer School on Particle Interactions at Very High Energies, Louvain, August 1973 [CERN preprint TH.1743 (1973)].
- 20) M.G. Olsson and E.T. Osypowski, to be published.

Figure captions

- Fig. 1 : The (3,3) phase shift with experimental points of J.R. Carter et al. (Ref. 10). The dashed curve is predicted by the naïve pole model with only the direct channel resonance. The solid curve is smoothly drawn to aid the eye.
- Fig. 2 : The dots represent the non-resonant background extracted from the experimental phase shifts of Fig. 1 using Eq. (36). The solid curve is the N exchange contribution to the background.
- Fig. 3 : a) Magnetic dipole Born term projection and resonance vertex factor N_M .
b) Electric quadrupole Born term projection and resonance vertex factor N_E .
- Fig. 4 : Phase angles ϕ_1^M and ϕ_1^E appearing in the photoproduction multipole formula (53). The angles ϕ_1 are given by $\phi_1 = \delta_p - \delta_e$, where δ_e is the elastic background phase due to N exchange.
- Fig. 5 : a) Real part of the magnetic dipole multipole M_{1+} . The curve represents the pole model prediction with the $\gamma N\Delta$ coupling constant $\kappa^* = 4.33$. The experimental points are from the analysis of Noelle et al. (Ref. 15).
b) Imaginary part of the magnetic dipole multipole M_{1+} again with $\kappa^* = 4.33$
- Fig. 6 : a) Real part of the electric quadrupole multipole E_{1+} . The curve represents the pole model prediction using only the Born term background. The experimental points are the analysis of Noelle et al. (Ref. 15).
b) Imaginary part of the E_{1+} multipole. Curve and data are described in Fig. 6a. Inclusion of the small Δ exchange contribution to the background will damp both the real and imaginary parts of E_{1+} above the resonance energy. The E_{1+} multipole is quite sensitive to the background, since in this case the resonance and background are of comparable magnitudes.

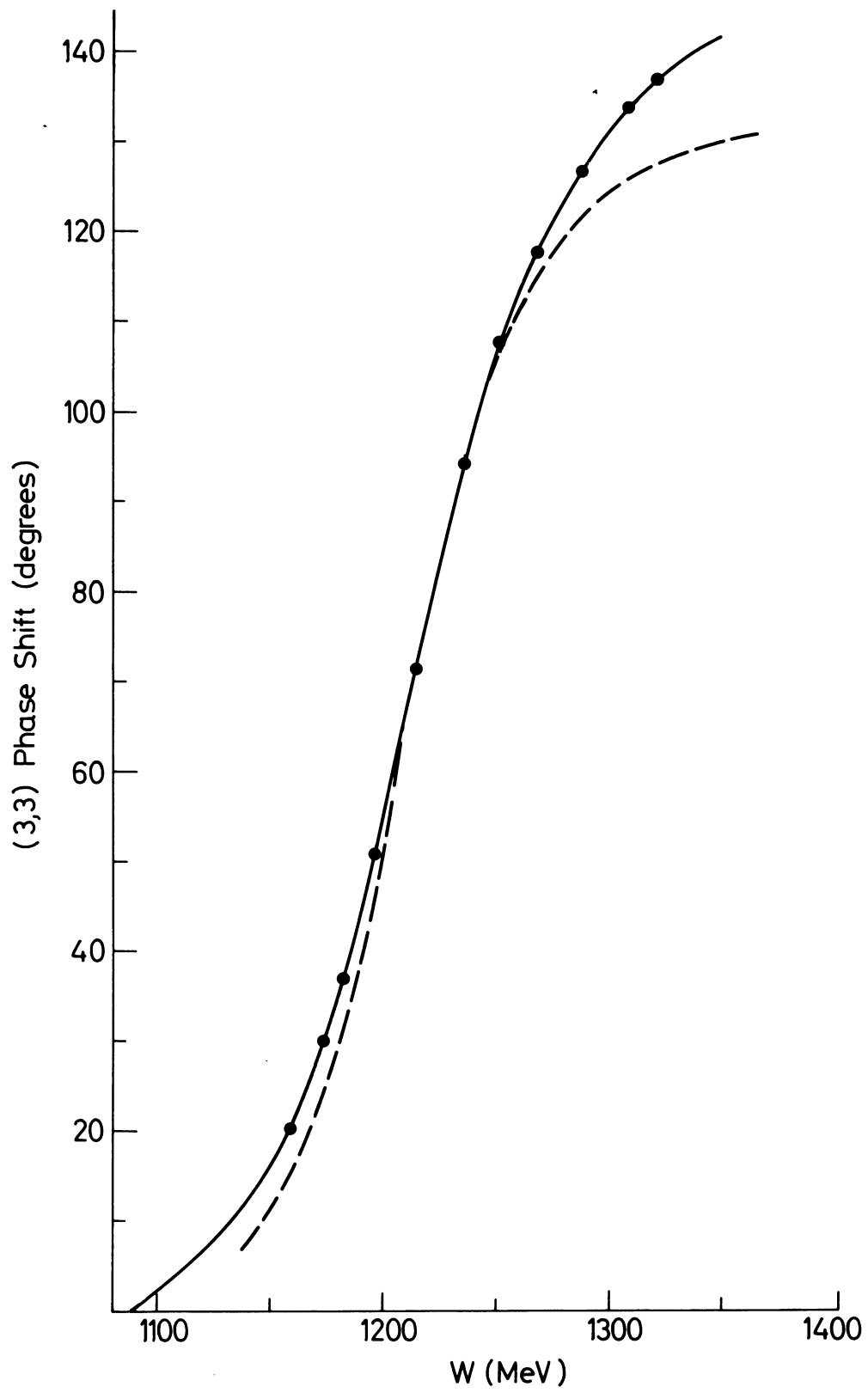


Fig. 1

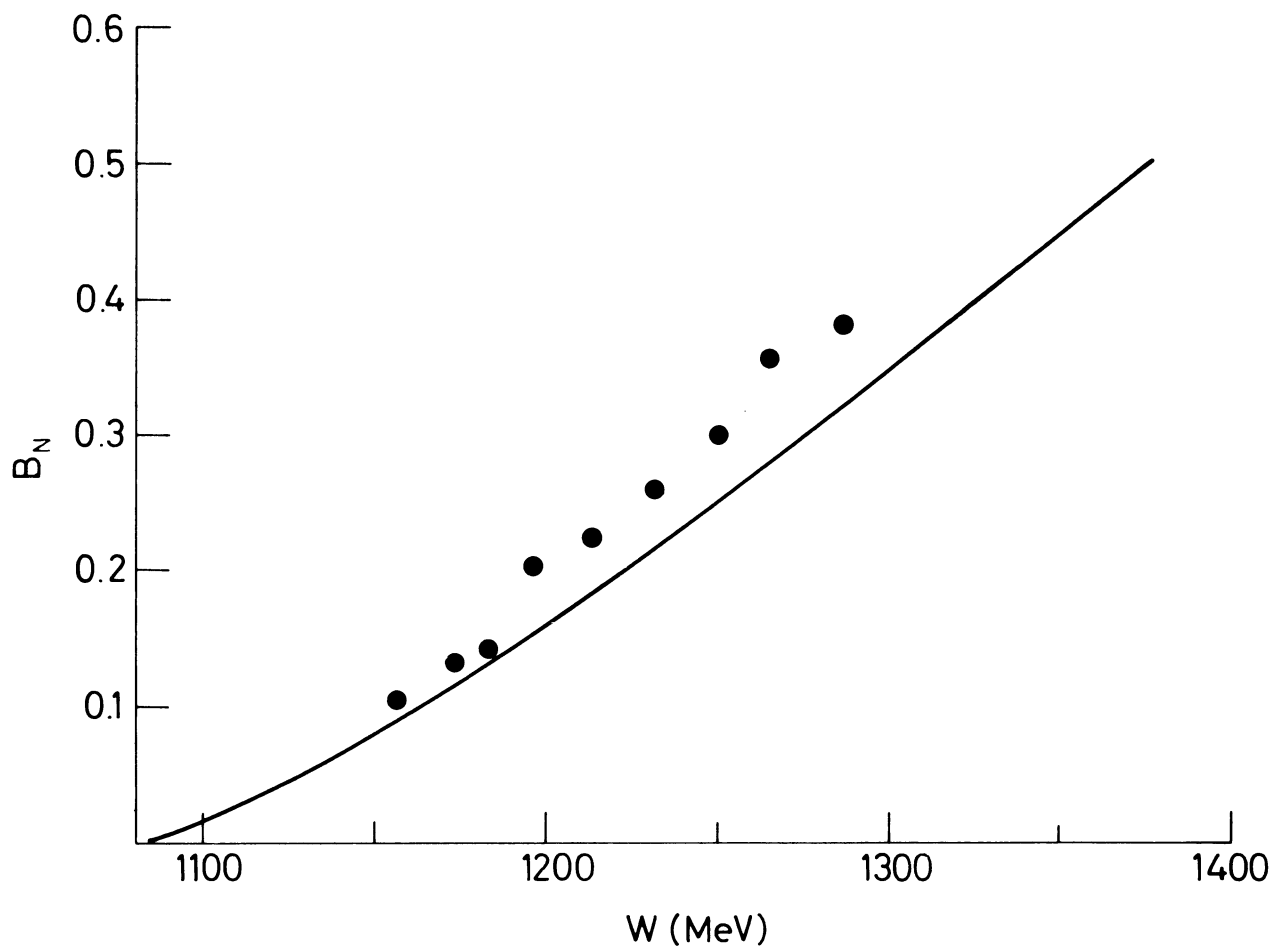


Fig. 2

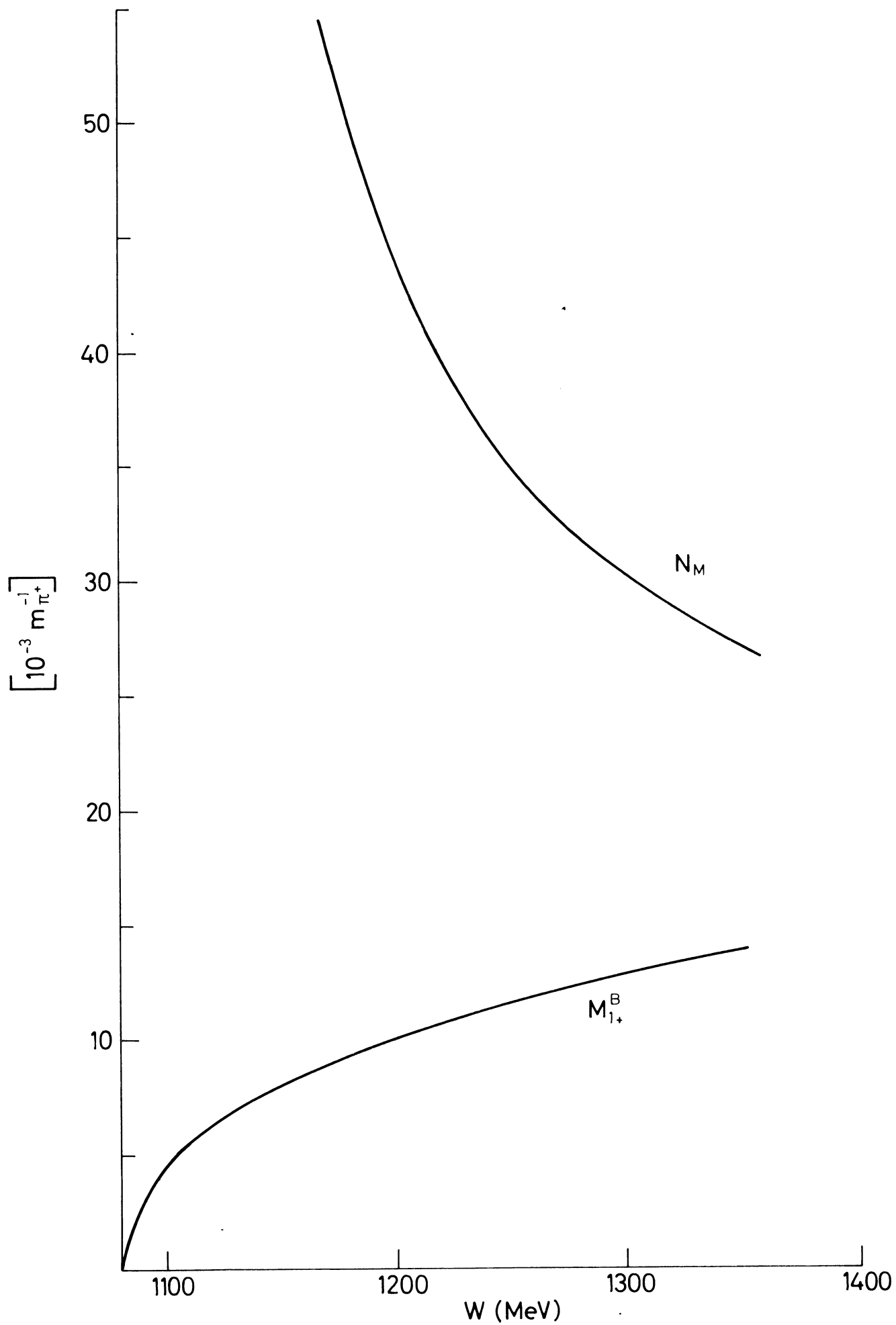


Fig. 3a

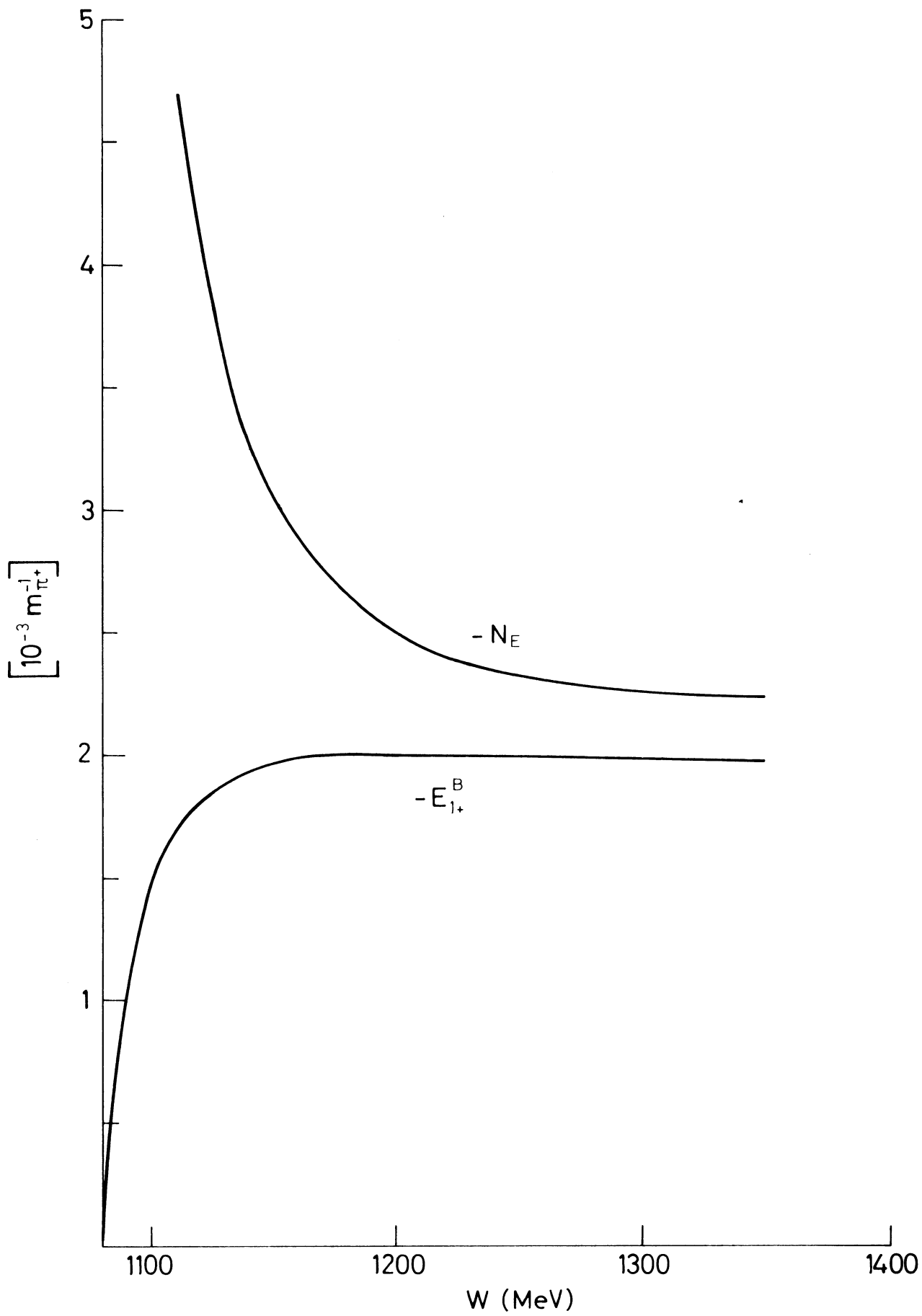


Fig. 3b

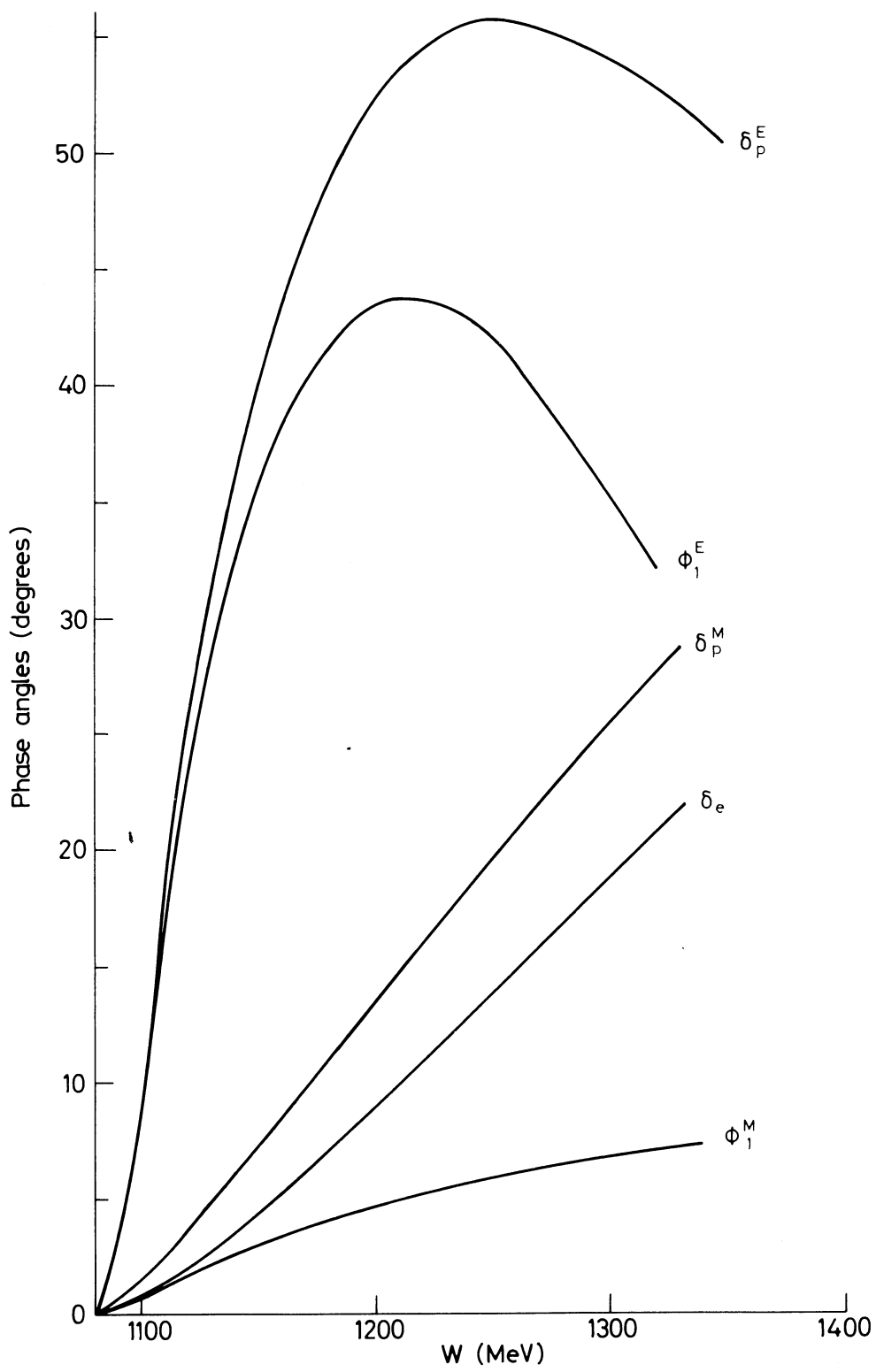


Fig. 4

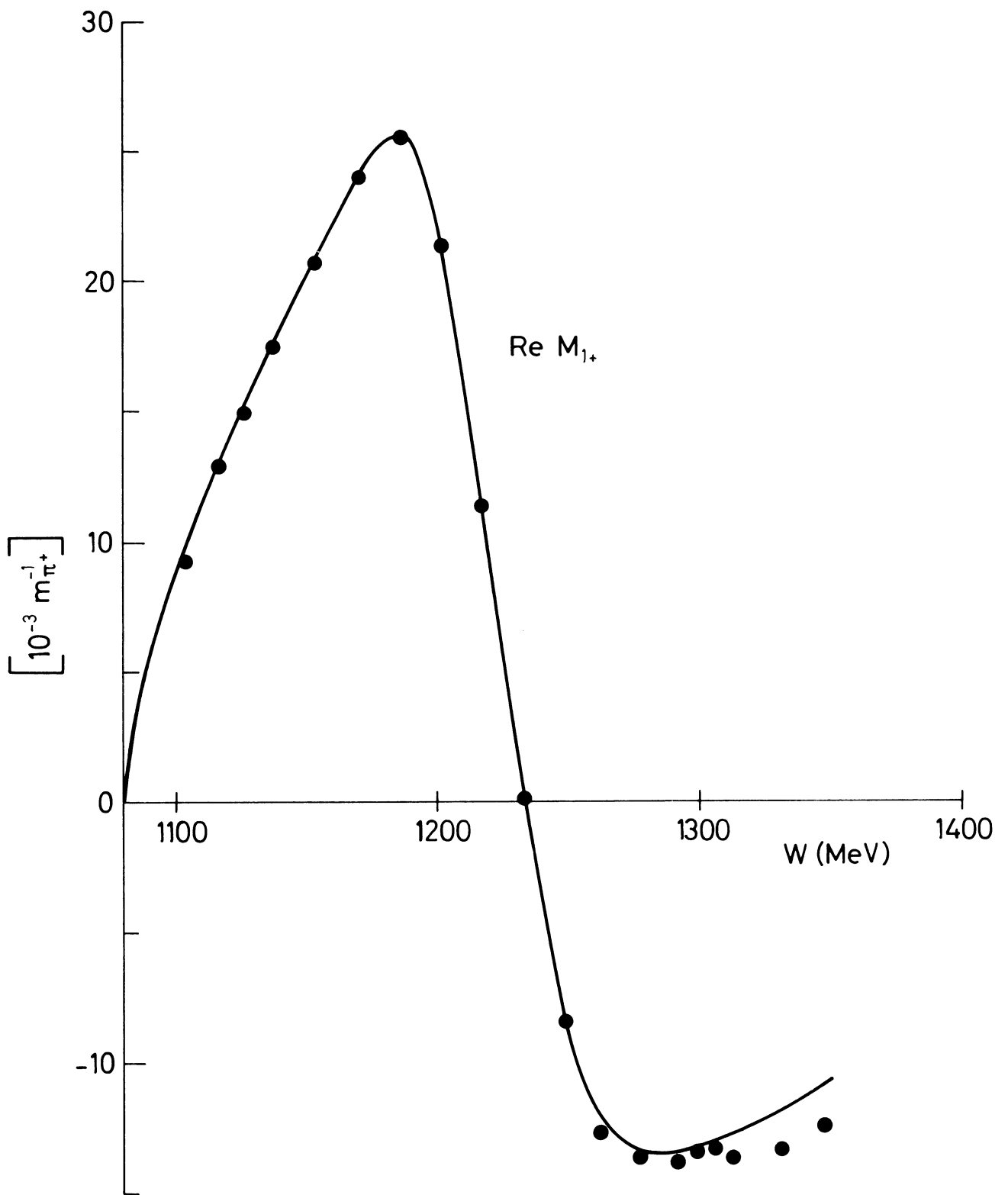


Fig. 5a

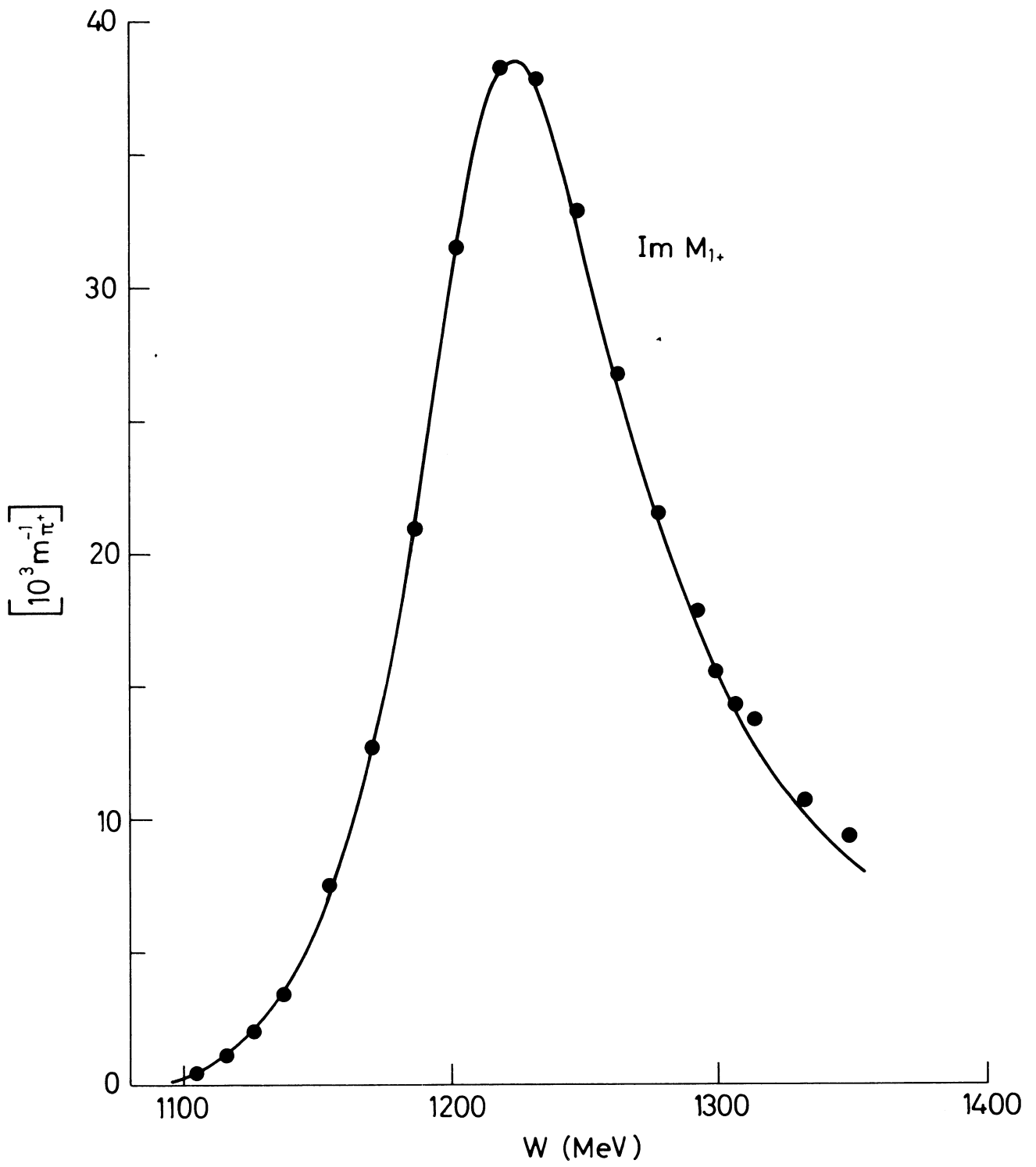


Fig. 5b

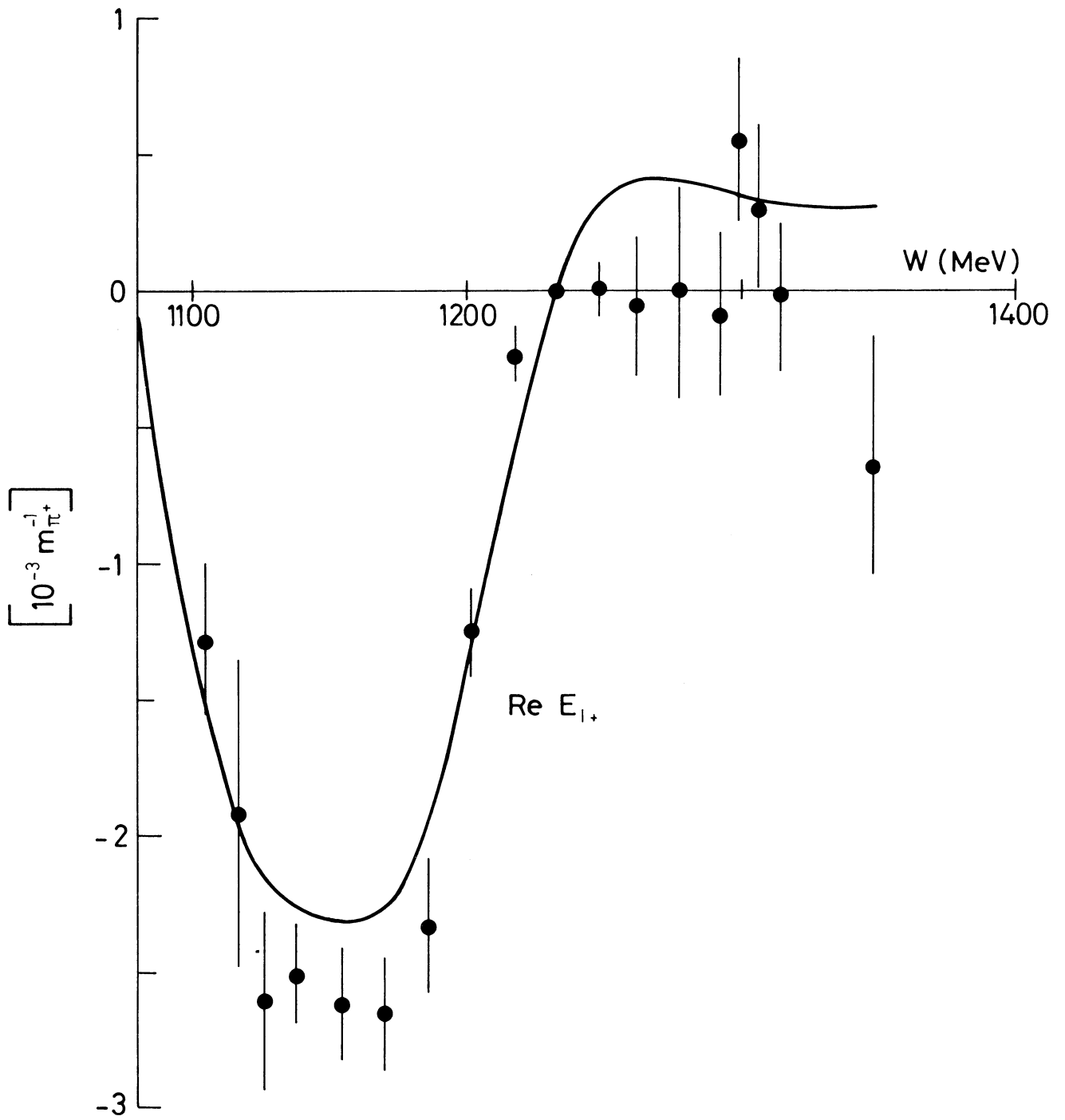


Fig. 6a

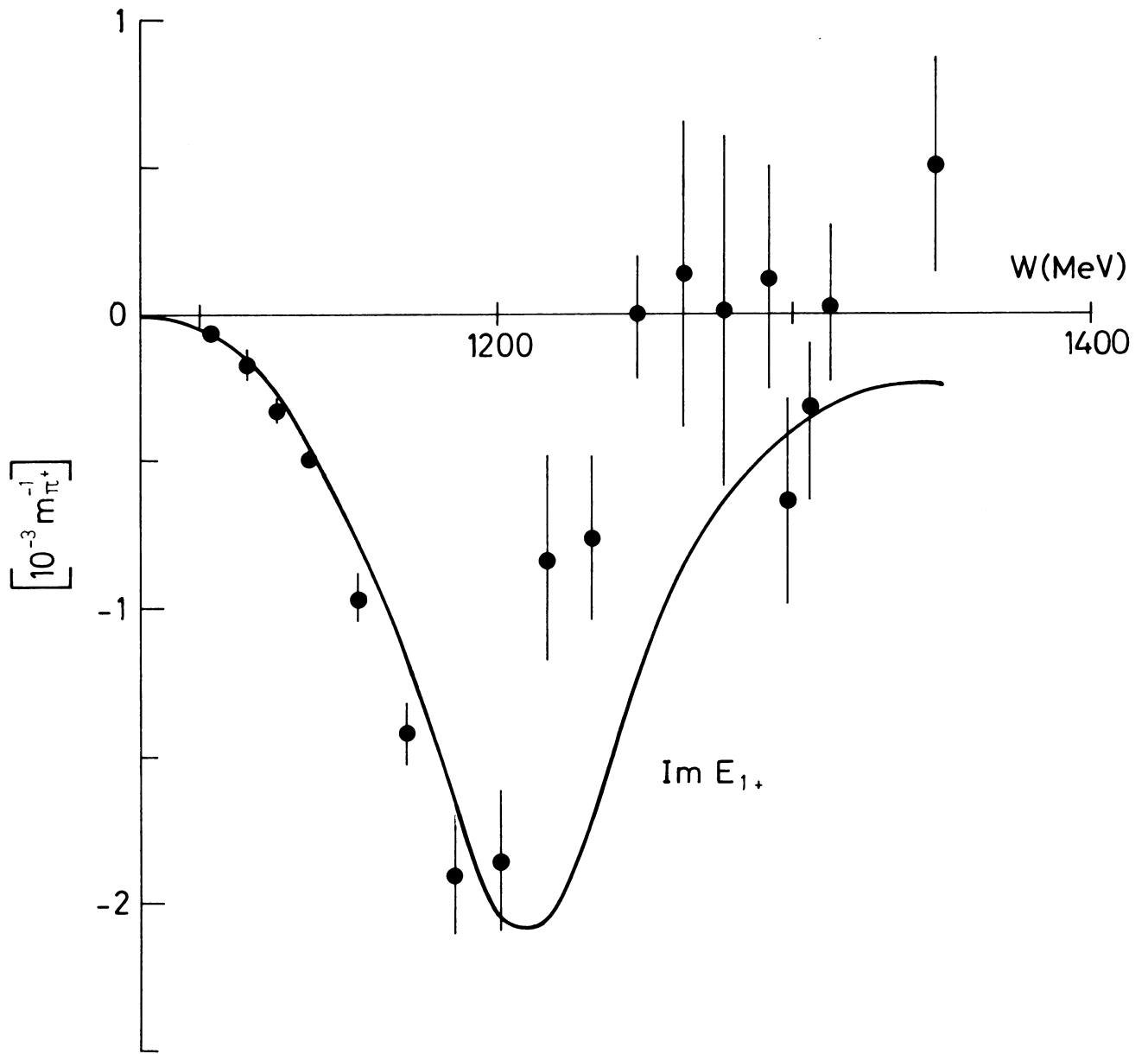


Fig. 6b